J. theor. Biol. (2002) **214,** 1–16
doi:10.1006/jtbi.2001.2400, available online at http://www.idealibrary.com on IDEAL®

Mathematical Modelling of Nitric Oxide Regulation of Rete Peg Formation in Psoriasis

NICHOLAS J. SAVILL*†, RICHARD WELLER‡ AND JONATHAN A. SHERRATT*

**Centre for Theoretical Modelling in Medicine, Department of Mathematics, Heriot–Watt University, Edinburgh EH14 4AS, U.K. and ‡Department of Surgery, UPMC, E 1557 Biomedical Science Tower, 200 Lothrop Street, Pittsburgh, PA 15261, U.S.A.*

(*Received on* 9 *November* 2000, *Accepted in revised form on* 16 *July* 2001)

Recent experiments have shown that in patients with psoriasis, highly elevated levels of nitric oxide (NO) are released at the surface of psoriatic plaques. Nitric oxide is a central biological regulator of many aspects of physiology, and it is a natural possibility that the high nitric oxide levels in psoriasis play a causal role in the onset of the disease. Here, we use mathematical modelling to investigate this possibility. We begin by discussing a simple model consisting of a single equation for nitric oxide concentration, which enables nitric oxide secretion rates in the basal epidermis to be calculated from the observed NO release rates at the skin surface. Using this key parameter value, we then develop an extended model that tests the hypothesis that nitric oxide regulates the formation of the extended rete pegs seen in psoriatic plaques. This occurs via the peroxynitrite-dependent activation of the collagenase MMP–8, which is produced by neutrophils present at high levels in psoriatic plaques. The plausibility of the hypothesis is demonstrated and specific testable quantitative predictions about the roles of the various cell types and signalling molecules are made.

1. Introduction

Nitric oxide has long been known as an environmental pollutant. But in the late 1980s it was also discovered to be a key physiological regulator, when a substance known previously as endothelium-derived relaxing factor was identified as nitric oxide (Ignarro *et al*., 1987). It was for this and related work that Furchgott, Ignarro and Murad were awarded the 1998 Nobel prize for physiology and medicine. Blood vessels dilate in response to nitric oxide, and blood flow is regulated by the production of nitric oxide by the endothelial cells lining blood vessels. This discovery was rapidly followed by the finding that nitric oxide was also responsible for the killing of bacterial cells by macrophages (Hibbs *et al*., 1989). In the last decade, there has been an explosion of experimental research on nitric oxide: it was named "molecule of the year" in 1992 by the journal *Science* (Culotta & Koshland Jr, 1992), and is now known to regulate biological function in most tissues in the body [see Moncada (1999) for review]. One of the many medical conditions in which nitric oxide may play a role is psoriasis.

Psoriasis is one of the world's most common skin diseases, affecting about 2% of the population; nevertheless, its biological cause is unknown. Normal skin consists of two layers: the epidermis, consisting of predominantly a single

†Author to whom correspondence should be addressed. E-mails: njs@ma.hw.ac.uk, wellerr@msx.upmc.edu, jas@ma.hw.ac.uk

0022–5193/02/010001 + 16 $35.00/0

close-packed cell type called keratinocytes and below this the dermis, composed of a collagen-based matrix within which reside fibroblast cells, blood vessels, nerve endings, and epidermal appendages such as hair follicles and sweat glands. The boundary between the epidermis and dermis has characteristic spatial oscillations known as rete ridges. In psoriasis, the epidermis is significantly thickened and poorly differentiated, causing flaking at the skin surface; it is also infiltrated by lymphocytes (white blood cells). The interface between the epidermis and dermis also changes, with very pronounced epidermal (rete) pegs protruding into the dermis [compare Fig. 1(a) and 1(b)]. In the most common form of psoriasis ("chronic plaque psoriasis"), these various changes occur in discrete plaques, separated by unaffected skin. These features characterizing psoriasis have all been known for many years, but the underlying molecular cause(s) of the disease remain unknown.

A recent development in the understanding of psoriasis has been the discovery that psoriatic plaques (a.k.a. lesions) actively produce nitric oxide. Kolb-Bachofen *et al.* (1994) first showed that epidermal keratinocytes in plaques produce the enzyme "inducible nitric oxide synthase", which is part of a nitric oxide production pathway, and Weller *et al.* (1996a) showed that nitric oxide synthesis is indeed increased in psoriasis. Healthy human skin does produce nitric oxide, at very low levels, as a result of chemical reactions within sweat (Weller *et al.*, 1996b). However, production is about ten times higher in non-lesional skin of psoriatics, and about ten times higher again in the plaques themselves (Weller & Ormerod, 1997; Orem *et al.*, 1997; Ormerod *et al.*, 1998). These observations are highly suggestive of a role for nitric oxide in the development of psoriasis, although no mechanism has yet been established. From a clinical viewpoint, this is an exciting possibility, because nitric oxide levels can be altered relatively easily, by topical application of nitric oxide donors or inhibitors. However, a detailed quantitative understanding of nitric oxide levels is an essential precursor to this, since the effects of nitric oxide are highly concentration-dependent.

In this paper, we begin (Section 2) by using a mathematical model to estimate nitric oxide concentrations within psoriatic plaques, based on experimental data on nitric oxide release rates at the skin surface. We then (Section 3) use an enlarged model to show how nitric oxide production can give rise to the characteristic pattern of pronounced rete pegs within the plaques. This is the first quantitative testable hypothesis for a plausible mechanism of rete peg formation. Mathematical modelling of nitric oxide in biology has a relatively long history. In 1994, Lancaster published a very influential paper in which he used a reaction–diffusion model to study the spatiotemporal distribution of nitric oxide around a single blood vessel; this has subsequently been refined and revised (Lancaster, 1997; Butler *et al.*, 1998; Vaughn *et al.*, 1998). Modelling has also been used to quantify the effects of nitric oxide donors (Schmidt *et al.*, 1997), to study the kinetics of nitric oxide's cytotoxic effects (Laurent *et al.*, 1996), and to investigate the potential role of nitric oxide in wound healing pathologies (Cobbold & Sherratt, 2000). By contrast, psoriasis has, to the best of our knowledge, not previously been studied using mathematical modelling.

2. Modelling Nitric Oxide Production in Psoriatic Plaques

The high production rates of nitric oxide in psoriatic plaques have been established by measuring release rates of nitric oxide from the skin surface. This involves a procedure, developed by Weller *et al.* (1996a), in which a nitrogen-filled vessel is placed over the skin surface, and the amount of nitric oxide collected over a prescribed time period (about 20 min) is measured by chemiluminescence. This procedure provides a quantitative comparison between nitric oxide production in different skin regions, different individuals, etc. However, it does not give direct information about the key issue of nitric oxide concentration levels within psoriatic plaques; our first modelling goal is to predict these concentrations.

Within psoriatic plaques, nitric oxide is secreted mainly by the basal layer of keratinocytes as observed by staining for iNOS (Kolb-Bachofen *et al.*, 1994; Ormerod *et al.*, 1998). We assume that the nitric oxide production rate is

uniform within the basal layer of the epidermis, and study the nitric oxide release rate at the skin surface that results from this. The model consists of a single partial differential equation for nitric oxide concentration $n(\underline{r}, t)$. We restrict the attention to a two-dimensional cross-section of the skin, illustrated schematically in Fig. 2, and assume uniformity in the third dimension; thus, $\underline{r} = (x, y)$ denotes a spatial position in two dimensions, and t denotes time. The definitions of the model's variables and parameters are given in Table 1 and a discussion of the parameter values is given in Appendix A.

The nitric oxide molecule is small and is soluble in phospholipid membranes and thus will diffuse at approximately the same (high) rate in different layers of the skin, unimpeded by cells, extracellular matrix components, etc. However, the reaction kinetics will be quite different for different regions. In the suprabasal epidermis, nitric oxide decays at a constant rate λ due to reactions with a range of free radicals (Lancaster, 1994). In the basal layer there is, in addition to this decay, production of nitric oxide at a rate a_1. Finally, within the dermis, the intrinsic decay rate is augmented by active scavenging of nitric oxide by blood, due to the rapid binding of nitric oxide to haemoglobin (Gow & Stamler, 1998). This is a key part of the model because it introduces an important nonlinearity; nitric oxide causes blood vessel dilation, which will in turn result in a higher volume of blood in the plaque, and thus more rapid removal of nitric oxide. We denote by $g(n)$ the increase in diameter of blood vessels relative to that in the healthy skin. Experimental data (Ku, 1996) indicate that an appropriate functional form is $g(n) = g_0 n/(g_1 + n)$ with $g_1 \approx 20$ nM.

The discussion implies the following form for our mathematical model:

$$\frac{\partial n}{\partial t} = D_n \nabla^2 n + \begin{cases} -\lambda n & \text{in suprabasal epidermis,} \\ -\lambda n + a_1 & \text{in basal layer,} \\ -\lambda n - d_1 n(1 + g(n)) & \text{in dermis.} \end{cases} \quad (1)$$

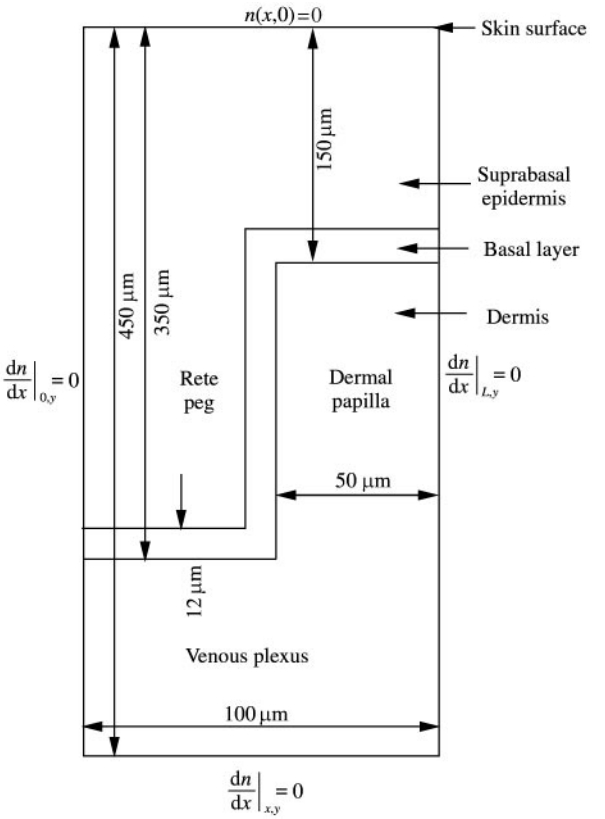

FIG. 2. Schematic illustration of the model set-up with boundary conditions and spatial dimensions. Basal cells make up roughly 30% of the cells in the rete pegs. In the model, the width of the basal cell layer needs to be about 12 μm in order to achieve this percentage coverage.

For the purposes of this section, we impose the divisions between these regions, based on the observed form of psoriatic plaques (Fig. 2). We consider the nitric oxide release rate at the skin surface over an area much larger than the intracapillary distance. Therefore, the spatial domain should be considered as an average over several square millimetres of skin. In the next section of the paper, we will go on to discuss the role played by nitric oxide in regulating the shape of the epidermal–dermal junction.

We solved eqn (1) on a rectangular domain with x and y coordinates parallel and perpendicular to the skin surface, respectively (see Fig. 2). The boundaries at $x = 0$ and L represent the centres of a rete peg and a dermal papilla, respectively, and no flux conditions are applied on these boundaries. Beyond the skin surface ($y = 0$) is air [or, in experimental measurement of nitric oxide release, a nitrogen-filled vessel

TABLE 1
Parameter definitions and values for the two models

Parameter	Description	Value
d_1	NO scavenging by Hb	$100\ s^{-1}$ ($10\ s^{-1}$ in model 1)
d_2	$ONOO^-$ reaction CO_2	$58\ s^{-1}$
d_3	$ONOO^-$ scavenging by Hb	$30\ s^{-1}$
d_4	ProMMP-8 decay	$0.01\ s^{-1}$
d_5	MMP-8 decay	$0.01\ s^{-1}$
d_6	Collagen degradation by fibroblasts	$100\ s^{-1}$
k_1	No reaction with O_2^-	$19\ nM^{-1}\ s^{-1}$
k_2	ProMMP-8 activation by $ONOO^-$	$10^{-5}\ nM^{-1}\ s^{-1}$
k_3	Collagen degradation by MMP-8	$5\times10^{-6}\ nM^{-1}\ s^{-1}$
a_1	NO production by basal cells	$170\ nM\ s^{-1}$
a_2L	ProMMP-8 production by neutrophils	$170\ nM\ s^{-1}$
a_3	Collagen production by fibroblasts	$5.36\times10^4\ \mu g\ mg^{-1}\ s^{-1}\ cell^{-1}\ \mu m^3$
D_n	NO diffusion coefficient in tissue	$3300\ \mu m^2\ s^{-1}$
D_p	$ONOO^-$ diffusion coefficient in tissue	$2600\ \mu m^2\ s^{-1}$
g_0	Maximal change in capillary cross-sectional area	9
g_1	[NO] for half-maximal change in capillary	20 nM
λ	NO removal in tissue	$0.17\ s^{-1}$
s	O_2^- concentration in tissue	0.01 nM
F	Fibroblast density in dermis	$10^{-8}\ cell\ \mu m^{-3}$
c_T	Threshold collagen density	$100\ \mu g\ mg^{-1}$
n	[NO]	
p	[$ONOO^-$]	
m'	[proMMP-8]	
m	[MMP-8]	
c	Collagen density	

Note: See Appendix A for details and references.

(Ormerod *et al*., 1998)]. The diffusion coefficient of nitric oxide in these media is about 1000 times greater than in biological tissues, and thus any nitric oxide released will diffuse away from the skin surface effectively instantaneously. Thus, the appropriate boundary condition at $y = 0$ is $n = 0$. The fourth boundary $y = Y$ is included for computational necessity; we use $\partial n/\partial y = 0$ as a boundary condition, but this is not significant provided that Y is sufficiently large.

Our aim is a quantitative solution of this model, and thus, good parameter estimates are essential; fortunately, there is a large literature on quantitative properties of nitric oxide on which these parameters can be based. The diffusion coefficient D_n of nitric oxide in tissue was measured as $3300\ \mu m^2\ s^{-1}$ by Malinski *et al.* (1993), using microsensor measurements. The parameter λ is the decay rate of nitric oxide in tissues due to reactions with free radicals, which is estimated as $0.17\ s^{-1}$, corresponding to a half-life of 4 s (Lancaster, 1994). The parameter d_1 can be estimated from the rate constant of nitric oxide binding to haemoglobin in flowing blood, which is $5\times10^4\ M^{-1}\ s^{-1}$ (Liao *et al*., 1999; note that the corresponding rate for free haemoglobin is about 1000 times larger). Blood vessels constitute about 10% of dermal papillae in a typical psoriatic plaque (Auer *et al*., 1994) so that a typical concentration of 2 mM (= 14 g per 100 ml) haemoglobin in the blood (Thibodeau & Patton, 1997) gives an average concentration of 0.2 mM in the dermal papillae. Thus, $d_1 = (5\times10^4)\times(0.2\times10^{-3})\ s^{-1} = 10\ s^{-1}$. We base the value of g_0 on estimates that blood flow in the dermal papillae of psoriatic plaques is between two and five times greater than in normal skin (Klemp & Staberg, 1983; Krogstad *et al*., 1995). Assuming Poiseuille flow in the vessels, this implies an increase in blood vessel area by factor of between 1.4 and 2.2 ($\sqrt{2}$–$\sqrt{5}$). Thus, the average value of $1 + g(n)$ in the dermal papillae dermis should be about 1.8.

The parameter g_0 can then be determined implicitly by numerical solutions of the model. This is done by calculating the average value of $g(n)$ in the dermal papilla, denoted by $\overline{g(n)}$.

The remaining parameter a_1 is estimated from numerical simulations of model (1), by the requirement that nitric oxide release rates at the skin surface correspond to those found experimentally for psoriatic plaques. Recent experiments by Richard Weller (manuscript in preparation) show an average release rate of $1.2\,\text{pmol}\,\text{cm}^{-2}\,\text{min}^{-1}$ from the surface of psoriatic plaques. Numerical solutions of model (1) rapidly evolve to a (spatially varying) steady state (Fig. 3), and the mean flux at the skin surface is easily calculated from this, as the average (over x) of $-D_n\partial n/\partial y$. We varied the parameters g_0 and a_1 in order to give the observed average values of increased blood flow in, and NO release from, psoriatic plaques; this gives values of $g_0 = 9$ (dimensionless) and $a_1 = 170\,\text{nM}\,\text{s}^{-1}$. Figure 4 illustrates the way in which the predicted nitric oxide release rate at the skin surface varies with a_1 and g_0; there is an approximately linear increase with a_1, while higher values of g_0 cause an increase in vascular scavenging of nitric oxide, and thus lower release rates. The inset shows how $1 + \overline{g(n)}$ varies with a_1 for a constant release rate of $1.2\,\text{pmol}\,\text{cm}^{-2}\,\text{min}^{-1}$. At $a_1 = 170\,\text{nM}\,\text{s}^{-1}$, $1 + \overline{g(n)} = 1.8$

This quantitative estimate of the parameter a_1 is an essential input to the modelling in the next section, which focuses on the regulation of the epidermal–dermal interface by nitric oxide. But the modelling in this section has important applications itself, because the model solutions for n are predictions of actual nitric oxide concentrations within the skin, something which is extremely difficult to measure experimentally. We predict that in psoriatic plaques, nitric oxide concentrations are about 0.05 nM near the skin surface, increasing to a maximum of about 10 nM in the middle of the rete pegs. These predictions provide natural benchmarking points for *in vitro* experiments on NO regulation of keratinocyte behaviour, which are possible, but to date have

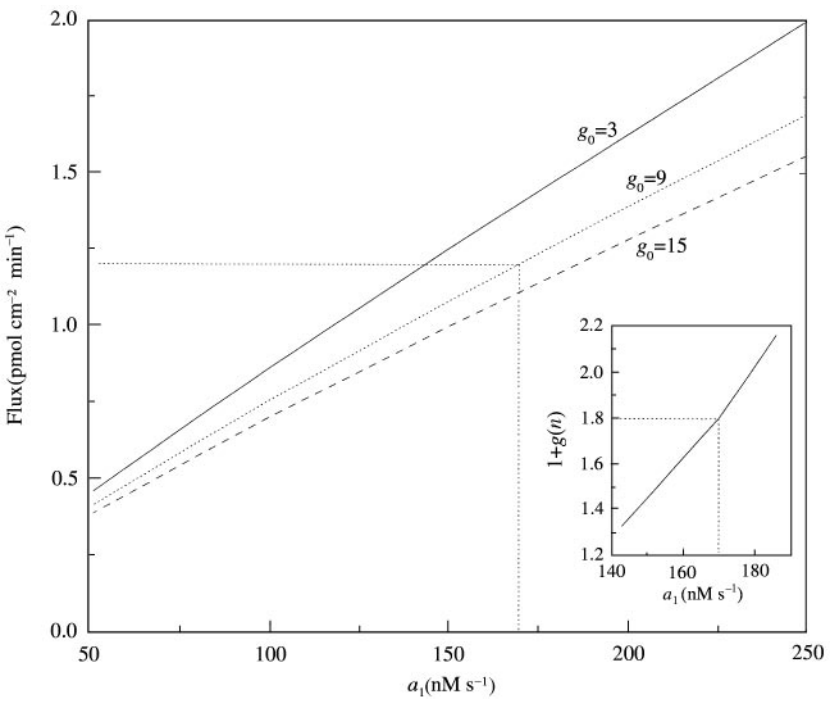

FIG. 4. The flux of nitric oxide at the skin surface from simulations of model 1 against the production rate, a_1 of nitric oxide by basal cells for various values of g_0. The flux is given by $-D_n\partial n/\partial x$, averaged over the full surface. The flux varies linearly with a_1 and declines for increasing values of g_0 representing greater dilation of blood vessels. At $g_0 = 9$ and $a_1 = 170\,\text{nM}\,\text{s}^{-1}$, the flux equals $1.2\,\text{pmol}\,\text{cm}^{-2}\,\text{min}^{-1}$, the average value is determined from the experiment. The inset shows how $1 + \overline{g(n)}$ varies for different a_1 at a constant flux of $1.2\,\text{pmol}\,\text{cm}^{-2}\,\text{min}^{-1}$.

been expressed in terms of concentrations of NO donors rather than nitric oxide itself (Krischel *et al.*, 1998).

3. Regulation of Rete Pegs by Nitric Oxide

Rete pegs extend from 50 to 500 μm into the dermis, their lower tips reaching the horizontal venous plexus (Bacharach-Buhles *et al.*, 1994a). Each dermal papilla contains a single tortuous capillary surrounded by ECM (Irwin *et al.*, 1977). At some locations, particularly at the tip of the dermal papillae, the capillary directly abuts the basal cell layer. The basal cells form an unbroken layer between the dermis and the other epidermal keratinocytes. In vertical sections of biopsies, the dermal papillae appear to have widely varying widths and sometimes appear as isolated islands surrounded by epidermis. This is an artifact of 2D sectioning of 3D finger-like structures, the islands occur because the axes of some papillae are oblique to the cut of the section. How these rete pegs and dermal papillae are formed is still unclear. Do the capillaries grow upwards into the dermis or does the epidermis grow down and around the capillaries? These two mechanisms are not mutually exclusive.

Capillary growth or angiogenesis is known to occur in psoriatic plaques; specifically, some endothelial cells in the vertical limbs of capillary loops label positively with the nuclear proliferation marker MAb MIB-1, while endothelial cells in non-lesional skin do not (Creamer *et al.*, 1997a). In addition, a plethora of angiogenic factors have been discovered in plaques (Ettehadi *et al.*, 1994; Elder *et al.*, 1989; Nickoloff *et al.*, 1994; Detmar *et al.*, 1994; Creamer *et al.*, 1997b; Bhushan *et al.*, 1999). Even though angiogenesis does occur, there is no evidence that it leads to capillary growth into the epidermis and there is no evidence of endothelial cell death in regressing plaques as one might expect (Braverman & Sibley, 1982). One possible effect of angiogenesis may be the observed capillary tortuosity (Bull *et al.*, 1992). Therefore, the evidence for angiogenesis is circumstantial at best.

Evidence in favour of epidermal growth into the dermis is stronger. Lymph capillaries and the horizontal subpapillary venous plexus are frequently observed to lie within some dermal papillae (Bacharach-Buhles *et al.*, 1994a, 1997). There is no evidence for or against lymphogenesis so this observation is still inconclusive (Cliff *et al.*, 1999). However, the second observation, if true, is a strong evidence for epidermal growth into the dermis. Another unexplained observation is the existence of ECM within dermal papillae: if the capillaries grow upwards into the dermis, how is the new ECM formed, or if the epidermis grows downwards, why does some of the ECM remain?

In this paper, we adopt the hypothesis put forward by Bacharach-Buhles *et al.* (1994a) that epidermis grows downwards and neglect any effect of angiogenesis. A future paper will consider angiogenesis as the rete peg formation mechanism. A model of the formation of rete pegs needs to account for the following. (i) The loss of ECM between capillaries over several weeks that causes the sinking of the basal layer into the dermis. (ii) The cessation of ECM loss giving a layer of ECM roughly 10 μm thick between the basal cells and the capillaries.

In order for the epidermis to grow between the capillaries, the ECM must be degraded faster than it is reformed by fibroblasts. Fibroblasts also degrade ECM; however, it is unlikely that they cause increased degradation because the normal turnover rate of ECM is on the order of several years (Uitto, 1986) and plaques develop within days. More likely candidates for the elevated degradation rates are the numerous neutrophils that infiltrate psoriatic plaques. Neutrophils migrate from the capillaries through the dermis and into the epidermis degrading both ECM and basement membrane. In resolving plaques, neutrophils disappear first, followed by the loss of dermal papillae and tortuous capillaries, suggesting that the fibroblasts reform the ECM once the neutrophils have left the plaque.

Assuming neutrophils are the cause of ECM loss, why does some ECM remain in the dermal papillae? If the epidermis moves downwards, this suggests that the ECM density at the epidermal–dermal junction is below a critical threshold such that basal cells are able to move into the degraded ECM. In a mature plaque, however, the ECM density at the junction should be at a critical threshold so that basal cells cannot move further into the ECM. Therefore, we need a factor (signalling molecule) that causes strong

neutrophil-induced ECM-degradation when the basal cells are far from the capillaries, but weakens degradation as the basal cells move closer to the capillaries. In addition, there must be a threshold density of ECM below which basal cells can move into the ECM.

A strong candidate for this factor is nitric oxide. Because basal cells are a source of nitric oxide and capillaries are a sink, the closer the basal cells are to the capillaries, the lower is the nitric oxide concentration within the dermis. Moreover, nitric oxide concentration determines the rate of neutrophil degradation of ECM: nitric oxide reacts rapidly with the free radical superoxide (O_2^-, a by-product of metabolism) to form peroxynitrite ($ONOO^-$). Peroxynitrite is a strong activator of neutrophil procollagenase (Okamoto *et al.*, 1997; Maeda *et al.*, 1998), the inactive form of collagenase secreted by neutrophils (also called MMP-8). These reactions can be represented as follows:

$$NO + O_2^- \xrightarrow{k_1} ONOO^-,$$

$$ONOO^- + \text{proMMP-8} \xrightarrow{k_2} \text{MMP-8},$$

$$\text{MMP-8} + \text{collagen} \xrightarrow{k_3} \text{MMP-8}.$$

Peroxynitrite, like nitric oxide, is a small and highly reactive free radical species, which therefore has a high diffusion coefficient and fast kinetics. MMP-8 is a 85 kDa molecule and is known to degrade collagen only in the locality of the secretory neutrophils due to its inhibition by tissue inhibitors of metalloproteinases (TIMPs).

The above reaction kinetics plus diffusion of nitric oxide and peroxynitrite can be written as a system of differential equations:

Nitric oxide:

$$\frac{\partial n}{\partial t} = D_n \nabla^2 n - \underbrace{k_1 s n}_{\substack{\text{reaction} \\ \text{with } O_2^-}} + \underbrace{\phi(n)}_{\substack{\text{production} \\ \text{and removal}}} \tag{2}$$

Peroxynitrite:

$$\frac{\partial p}{\partial t} = D_p \nabla^2 p + \underbrace{k_1 s n}_{\substack{\text{reaction} \\ \text{with } O_2^-}} - \underbrace{d_2 p}_{\text{decay}} + \underbrace{\psi(n, p, m')}_{\text{removal}} \tag{3}$$

Procollagenase:

$$\frac{\mathrm{d}m'}{\mathrm{d}t} = \underbrace{-k_2 p m'}_{\text{activation}} - \underbrace{d_4 m'}_{\text{decay}} + \underbrace{a_2 L}_{\substack{\text{production} \\ \text{by neutrophils}}} \tag{4}$$

Collagenase:

$$\frac{\mathrm{d}m}{\mathrm{d}t} = \underbrace{k_2 p m'}_{\text{activation}} - \underbrace{d_5 m}_{\text{decay}} \tag{5}$$

Collagen:

$$\frac{\mathrm{d}c}{\mathrm{d}t} = \underbrace{a_3 F}_{\substack{\text{secretion} \\ \text{by fibroblasts}}} - \underbrace{k_3 m c}_{\substack{\text{breakdown} \\ \text{by collagenase}}} - \underbrace{d_6 F c}_{\substack{\text{breakdown} \\ \text{by fibroblasts}}} \tag{6}$$

where

$$\phi(n) = \begin{cases} a_1 & \text{in basal layer,} \\ -d_1 n(1 + g(n)) & \text{in capillaries,} \\ 0 & \text{otherwise,} \end{cases}$$

and

$$\psi(n, p, m') = \begin{cases} -k_2 p m' & \text{in ECM,} \\ -d_3 p(1 + g(n)) & \text{in capillaries,} \\ 0 & \text{otherwise.} \end{cases}$$

The variables n, p, m' and m are the molar concentrations of nitric oxide, peroxynitrite, procollagenase and collagenase, respectively, and c is the dry weight density of collagen. Nitric oxide dynamics are as in Section 2, except that the parameter λ has been replaced by $k_1 s$, where s is the constant molar concentration of superoxide. As discussed above, the reaction of nitric oxide with superoxide produces peroxynitrite, which has a constant background removal rate (d_2), primarily by reaction with carbon dioxide, and is also removed actively (modelled by the function ψ). They key property of peroxynitrite is its activation of procollagenase (rate constant k_2), which is produced at a constant rate a_2 by neutrophils (density L). Both pro and active forms of collagenase have intrinsic decay rates, denoted by d_4 and d_5, respectively; d_5 incorporates the effects of TIMPs. The final equation represents collagen production by fibroblasts (density F) and removal both by active collagenase and by fibroblasts

(which will produce different types of collagenase). The explicit spatial dependence in the model is only through the diffusion of nitric oxide and peroxynitrite, with coefficients D_n and D_p, respectively. The nitric oxide and peroxynitrite concentrations are defined over the whole spatial domain, i.e. within the epidermis, ECM and the capillaries. The procollagenase, collagenase and collagen are defined where the collagen density is greater than the threshold collagen density, i.e. where $c > c_T$. The speed of neutrophil and fibroblast migration through the ECM is roughly 15 μm h^{-1} (Friedl *et al.*, 1998). This is much faster than the movement of the epidermis into the dermis. Hence, we assume that the time averaged density of neutrophils and fibroblasts is constant.

As in Section 2, we attempt a quantitative solution of the model, and all the parameters in the model are either known or can be estimated from *in vitro* experiments or via theoretical considerations; details are given in Appendix A.

3.1. ANALYSIS OF THE MODEL

We first analyse the model in order to study its general behaviour. The equations for the free radicals are coupled to the other three equations by the term $k_2 p m'$. Fortunately, as we will show in Section 3.3, this term is negligible with respect to the other terms in eqn (3). Dropping this term means we can solve the free radical equations independently from the others. Unfortunately, there are no analytical solutions for the free radical equations. However, the free radical dynamics are very fast compared to the degradation of collagen. Hence, we can find their spatial equilibrium solutions (denoted by $n^*(\underline{r})$ and $p^*(\underline{r})$) and substitute these values into the remaining set of ordinary differential equations. The equilibrium concentrations of procollagenase, collagenase and collagen for a given equilibrium concentration of peroxynitrite can be found by setting the left-hand sides of eqns (4)–(6) to zero. These are given by

$$m'^* = \frac{a_2 L}{d_4}, \tag{7}$$

$$m^* = \frac{k_2 a_2 L}{d_4 d_5} p^*, \tag{8}$$

$$c^* = \frac{\alpha}{\beta p^* + 1} \tag{9}$$

assuming that $k_2 p^* \ll d_4$ (see Section 3.2), where

$$\alpha = \frac{a_3}{d_6}, \qquad \beta = \frac{k_2}{d_4}\left(\frac{k_3 a_2 L}{d_5 d_6 F} + 1\right).$$

From Table 1 we have $k_3 a_2 L/(d_5 d_6 F) = 85\,000 \gg 1$ hence

$$\beta = \frac{k_2 k_3 a_2 L}{d_4 d_5 d_6 F} = 85 \text{ nM}^{-1}. \tag{10}$$

These equations predict that the procollagenase concentration (m'^*) is roughly constant throughout the dermis and remains thus as the plaque develops. The collagenase concentration (m^*) depends linearly on peroxynitrite concentration and hence declines as the epidermal–dermal junction moves closer to the capillaries. The form of eqn (9) is shown in Fig. 5. The collagen density in normal skin ($p^* \approx 0$) is given by $\alpha = 536$ μg mg^{-1} (Shah *et al.*, 1994). The collagen

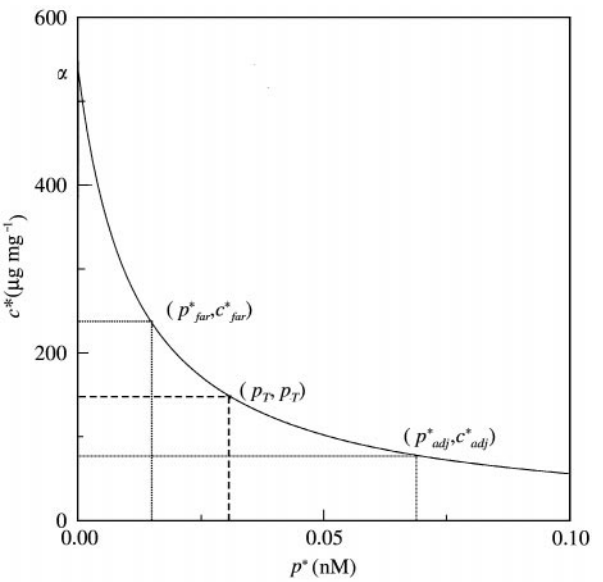

FIG. 5. The equilibrium collagen density is inversely proportional to the equilibrium peroxynitrite concentration [eqn (9)]. In normal skin $p^* \approx 0$ and $c^* \approx \alpha$. The half-normal collagen density occurs when $p^* = \beta^{-1}$. p_T is the peroxynitrite concentration at the epidermal–dermal junction when the collagen density is at threshold, c_T. c^*_{far} is the collagen density at the epidermal–dermal junction when the basal cells are far from the capillaries (defined as 85 μm in the 1D simulations). c^*_{adj} is the collagen density at the epidermal–dermal junction when the basal cells abut the capillaries.

density approaches zero as $p^* \to \infty$, and the half-normal density is given when $p^* = \beta^{-1} =$ 0.012 nM.

The key idea underlying our hypothesized mechanism of rete peg formation is that collagen density will be high near the capillary, but will decrease rapidly away from the capillary, enabling the epidermis to invade. We hypothesize that this gradient in collagen occurs in response to that in peroxynitrite, which will decrease significantly near a capillary, due to haemoglobin scavenging of nitric oxide and peroxynitrite. With this mechanism in mind, eqn (9) gives important quantitative insights. For the model to reproduce rete pegs the peroxynitrite concentration when the basal cells are far from the capillaries should be large enough to reduce the collagen density at the epidermal–dermal junction to below the threshold collagen density (i.e. $c^*_{far} < c_T$ and $p^*_{far} > p_T$, see Fig. 5). As the junction moves closer to the capillaries the peroxynitrite concentration decreases due to scavenging of peroxynitrite and nitric oxide by haemoglobin, and the collagen density at the epidermal–dermal junction rises. If the collagen density reaches the threshold density before the basal cells reach the capillaries, then rete peg formation stops and each dermal papilla contains a single capillary surrounded by ECM (i.e. $c^*_{adj} > c_T$ and $p^*_{adj} < p_T$). Two other cases are possible. (i) When $c^*_{far} > c_T$, then no rete pegs will form and (ii) when $c^*_{adj} < c_T$, then the basal cells will directly abut the capillaries.

From a therapeutic viewpoint the parameter β is very interesting. A reduction in its value means that more peroxynitrite is needed to give the same reduction in collagen density. Therefore, any physiological change to any of the parameters in eqn (10) that decrease β would have a negative effect on rete peg formation. Good candidates reduce the neutrophil density and increase the fibroblast density, both of which can be controlled. The other therapeutically accessible variable is peroxynitrite concentration, via nitric oxide depletion by NO-inhibitors.

3.2. ONE-DIMENSIONAL SIMULATIONS

Detailed simulation of rete peg formation in the model (2–6) requires a simulation in two spatial dimensions; however, we have been unable to solve the full model in 2D because of computational constraints. Therefore, we begin by solving the full model in a one-dimensional analogue of rete peg formation, before solving (Section 3.3) a simplified system of equations in two space dimensions. Our one-dimensional formulation consists of a finite domain of length 100 μm, with a 5 μm region at the bottom boundary corresponding to a capillary. The basal cells are modelled as a 12 μm wide movable region, initially placed at the top boundary. As the solution evolves, we check the collagen density at the epidermal–dermal junction, and if this is below the critical threshold c_T, the basal cells are shifted towards the capillary until the density at the junction is at the threshold. Initially, all variables are set to 0 except the collagen density which is set to a_3/d_6 in the dermis, and there are zero flux end conditions on both boundaries.

A typical 1D simulation over a period of 12 days is shown in Fig. 6. Time runs from left to right and space runs from top to bottom. The nitric oxide and peroxynitrite concentrations equilibrate within a few seconds due to their fast diffusion and kinetics. The procollagenase and collagenase equilibrate within several minutes and the collagen density equilibrates over several days. Figure 7 shows how the spatial distribution of the variables changes as the basal layer moves closer to the capillary. Each curve is a snapshot in time taken every 10^5 s. The arrows at the top of each graph show the position of the epidermal–dermal junction at each snapshot. At the capillary ($x = 95$ μm), all variables except collagen change very little as the basal cells move closer. The peroxynitrite concentration is always appreciable leading to some degradation of collagen at the capillary.

The story is different at the epidermal–dermal junction. As the basal layer moves closer, both nitric oxide and peroxynitrite concentrations fall due to their scavenging by haemoglobin. They decrease almost linearly with distance due to their high diffusion coefficients. The procollagenase concentration is high (at μM levels) due to a large production by neutrophils and slow activation by peroxynitrite [eqn (7)]. Its concentration changes very little because its activation is slower than its degradation ($k_2 p^* \ll d_4$). The

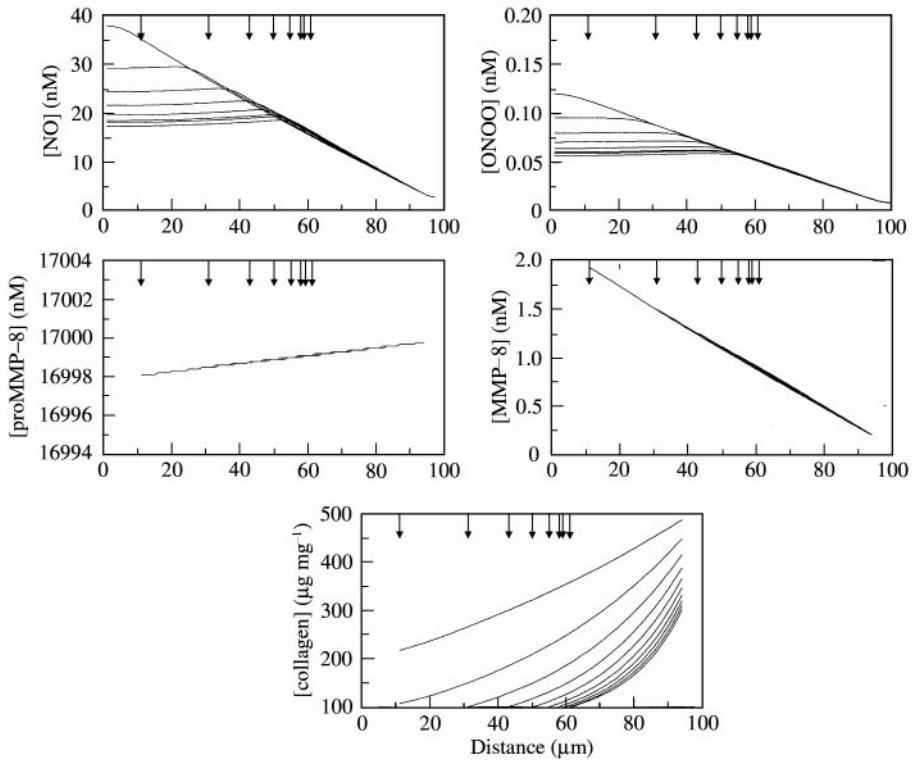

FIG. 7. Snapshots of the spatial concentrations of the solutions of eqns (2–6) taken every 10^5 s from Fig. 6. The arrows denote the position of the epidermal–dermal junction at the time of each snapsot. Initially, the epidermal–dermal junction is at position 12 μm and the edge of the capillary is at position 95 μm. The simulation details are as in Fig. 6.

collagenase concentration (defined only in the dermis) falls linearly due to its linear relationship with peroxynitrite [eqn (8)]. The collagen concentration initially falls from its normal density of a_3/d_6 to the critical threshold density c_T, where it remains throughout the development of the plaque.

As discussed in Section 3.1 the condition for rete peg formation with ECM remaining within the dermal papillae is $c^*_{far} < c_T < c^*_{adj}$ or $p^*_{adj} < p_T < p^*_{far}$. The peroxynitrite concentration is determined by the production and decay of nitric oxide, its conversion into peroxynitrite and scavenging by haemoglobin. The collagen density for a given peroxynitrite concentration is given by eqn (9) while the important parameter determining its behaviour is β. We have estimates for all these parameters except c_T. To examine the robustness of the model to parameter changes we first solved the nitric oxide and peroxynitrite equations independently of the others for different parameter values (Table 2). From the experimental work of Malinski *et al.* (1993), Vaughn *et al.* (1998) estimated the nitric oxide diffusion coefficient to lie between 2000 and 3400 μm^2 s^{-1}. They also estimated the nitric oxide removal rate in tissue to be about 0.01 s^{-1}, which is an order of magnitude smaller than that given by Lancaster (1994). We then examined two cases, firstly, when the basal cells were far from the capillaries (85 μm) and secondly, when the basal cells directly abut the capillaries. These two cases provide values for the peroxynitrite concentration at the epidermal–dermal junction i.e. p^*_{far} and p^*_{adj}, respectively. We then plotted the values of c^*_{far} and c^*_{adj} against β using eqn (9) for which rete peg formation would occur (Fig. 8). For a given β, if $c_T < c^*_{far}$ (lower curve) then the collagen density never falls below the threshold density and rete pegs will not form. If $c_T > c^*_{adj}$ (upper curve), then the basal cells will directly abut the capillaries. If c_T lies between c^*_{far} and c^*_{adj}, then rete pegs will form with ECM remaining in the dermal papillae. The graphs show that if $\beta^{-1} \sim 100$, then

TABLE 2
Changes in parameters for robustness tests

D_n	s	d_1	a_1	p^*_{adj}	p^*_{far}	Figure 8
3300	0.17	100	170	0.0075	0.11	A
3300	0.17	200	204	0.0071	0.13	B
3300	0.017	100	132	0.00064	0.010	C
2000	0.17	100	247	0.011	0.23	D

Note: The nitric oxide production rate by basal cells was adjusted to maintain a release rate of 1.2 pmol cm^{-2} min^{-1} at the skin surface for the parameter changes given. The peroxynitrite concentrations at the epidermal–dermal junction are given when the basal cells are far from the capillaries (85 μm) and when they are adjacent to the capillaries.

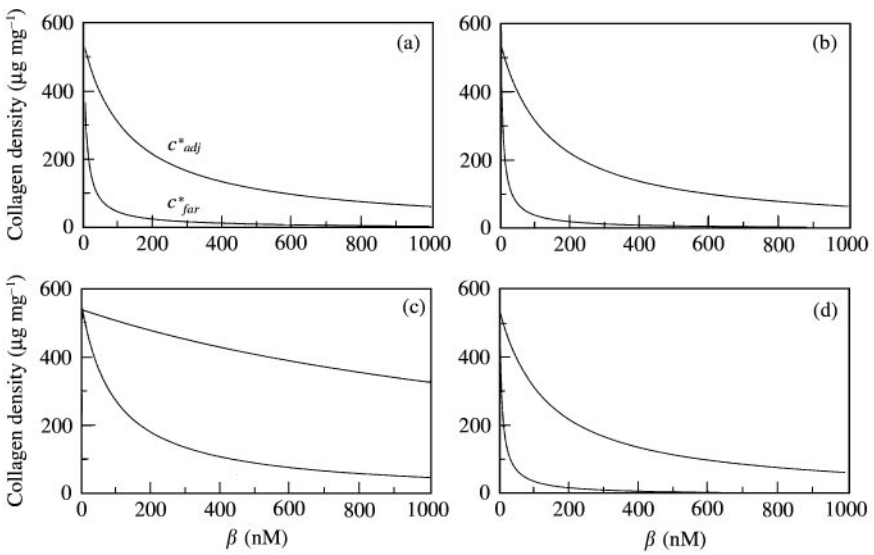

FIG. 8. Parameter robustness. For a given set of free radical parameters, peroxynitrite concentrations are calculated from the 1D simulations at the epidermal–dermal junction when the basal cells are far from the capillaries (85 μm) and when they are adjacent to the capillaries (i.e. p^*_{far} and p^*_{adj}, respectively). We then plot the collagen densities, c^*_{far} and c^*_{adj} against β. If $c_T < c^*_{far}$ no rete pegs will form, if $c^*_{far} < c_T < c^*_{adj}$ rete pegs will form with ECM in the dermal papillae and if $c_T > c^*_{adj}$ there will be no ECM between the basal cells and the capillaries. The four figures correspond to the parameter changes given in Table 2.

there is a large range of values of c_T which gives rete peg formation with ECM in the dermal papillae. The closer the c_T is to the upper curve, the more pronounced the rete pegs become and the lesser the ECM is in the papillae. For larger values of β^{-1}, values for c_T become more restricted. We estimate β^{-1} to be about 85 nM. Changes in the diffusion coefficient and the nitric oxide scavenging rate by haemoglobin make very little difference to peroxynitrite concentration (Table 2) and thus little difference to c^*_{far} and c^*_{adj} [cf. Fig. 8(a, b, d)]. However, an order of magnitude reduction in superoxide concentration or nitric oxide removal rate decreases peroxynitrite concentration by an order of magnitude [Fig. 8(c)]. This increases the size of the c_T/β^{-1} parameter region for which rete peg formation occurs. Although for $\beta = 85$ nM the range for c_T shifts to higher values.

3.3. TWO-DIMENSIONAL SIMULATIONS

In two dimensions it is not possible to simultaneously solve all the equations because large

differences in time-scales between nitric oxide and collagen dynamics cause prohibitively long simulation times. However, it is possible to decouple the equations and hence simulate them independently as discussed in Section 3.2. The 1D simulations show that the term $k_2 pm'$ is of the order 10^{-2}, whereas the term $k_1 sn$ is of the order 1 and the terms $d_2 p$ and $d_3 p(1 + g(n))$ are of the order 10 (units of $\mathrm{nM\,s^{-1}}$). Therefore, the term $k_2 pm'$ can reasonably be neglected, and the equations for nitric oxide and peroxynitrite then become independent of the other three. Moreover, the equations for procollagenase and collagenase are independent of the equation for collagen. Hence, we can simulate the fast equilibration of nitric oxide and peroxynitrite, then analytically calculate the equilibrium concentrations of procollagenase and collagenase by setting the LHS of their equations to 0. Finally, we can then simulate the degradation of collagen over time, moving the epidermal–dermal junction so that there is the collagen density at the critical threshold value. With the new configuration of basal cells, the nitric oxide and peroxynitrite equilibrium concentrations can be recalculated and the processes repeated until no further movement of the basal cells occurs.

Figure 9 shows one such simulation. The basal cells are modelled as a 12 μm wide movable region, initially placed 100 μm below the skin surface. The capillaries are 10 μm wide, and we have arbitrarily chosen their configuration to demonstrate the robustness of the pattern forming mechanism. The boundary conditions are as in Section 2. Figure 9(a) shows the initial configuration of capillaries and basal layer with equilibrium concentrations of nitric oxide and peroxynitrite. The density of collagen at the epidermal–dermal junction has just dropped below the critical threshold and a new configuration of the basal layer is just about to be calculated. Figure 9(b) shows the final configuration of basal cells, where no more movement is possible. This final pattern closely resembles the configurations seen in psoriatic plaques [see Fig. 1(b)].

4. Conclusion

In this paper, we have presented two different models related to nitric oxide activity in psoriasis. The first model assumes a fixed skin geometry, and predicts nitric oxide density within, and release from, the skin, as a result of production in the basal epidermis. Using data on nitric oxide release rates from psoriatic plaques, this model predicts an NO production rate by basal epidermal cells of about $170\ \mathrm{nM\,s^{-1}}$. Within the tissue, NO concentrations reach about 10 nM and at the skin surface about 0.05 nM. We found no experimental reports on NO production rates from basal epidermal cells nor any data on NO concentrations within psoriatic plaques. Vaughn *et al.* (1998) have estimated from the work of Malinski *et al.* (1993) an NO production rate by endothelial cells about an order of a magnitude larger than our estimate for basal epidermal cells.

Building on this, the second model considers the regulation, by nitric oxide, of the interface between the epidermis and dermis. This model predicts that the NO production in the basal epidermis can cause the formation of the pronounced rete pegs seen in psoriatic plaques. We hypothesize that the basic mechanism for this is the rapid conversion of NO to peroxynitrite, which in turn regulates the activation of procollagenase secreted by neutrophils. As the collagen degrades the basal cells and the epidermis move closer to the capillaries. At a critical collagen density, basal cells can no longer move into the ECM thus halting their movement and creating the rete pegs and dermal papillae observed in the psoriatic plaques. From the estimated parameter values from the literature we have shown that this is a plausible model that is robust to changes in parameter values. A critical parameter in the model is β which relates collagen density in the ECM to the peroxynitrite concentration. Because β depends on many of the model's parameters we can quantitatively predict how changes in these parameters affect rete peg formation.

From *in vitro* experimental work on collagen degradation (Okamoto *et al.*, 1997) we predict a procollagenase activation rate by peroxynitrite of $10^{-5}\ \mathrm{nM^{-1}\,s^{-1}}$ and a collagen degradation rate by collagen of $5 \times 10^{-6}\ \mathrm{nM^{-1}\,s^{-1}}$. The depth of the rete pegs depends on how a collagen density at the epidermal–dermal junction varies with peroxynitrite concentration (Fig. 5) and on the

collagen density threshold below which the epidermis can invade the dermis.

We have focussed on the role of nitric oxide in controlling the formation of highly pronounced rete pegs in psoriasis. However, nitric oxide is also a potential regulator of a number of other aspects of cell behaviour, which may play a role in psoriasis, in particular the growth and differentiation of keratinocytes (Krischel *et al*., 1998) and the endothelial cell growth and migration (Ziche *et al*., 1994). Detailed studies of the effects of these activities of nitric oxide in psoriasis are essential before a full assessment can be made of the overall role of nitric oxide in the onset of the disease. This is a natural area for future mathematical modelling.

From a therapeutic viewpoint, the suggestion that nitric oxide may play a causal role in psoriasis is an exciting one, because nitric oxide levels can be altered by topical application of creams containing either NO-donors or NO-inhibitors. In fact, a study has recently been published in which an NO-inhibitor was applied topically in psoriasis: NO release was reduced, but with no effect on clinical outcome (Ormerod *et al*., 2000). However, because the effects of nitric oxide are so concentration-dependent, it is quite possible that different treatment regimes may be successful. Our research forms a part of a growing body of work providing, for the first time, clues to the underlying molecular causes of psoriasis, and this has the potential to lead to a new generation of anti-psoriasis therapies.

NJS and JAS are supported in part by SHEFC Research and Development grant 107 "Centre for Theoretical Modelling in Medicine". JAS is supported in part by an EPSRC Advanced Research Fellowship.

REFERENCES

AUER, T., BACHARACH-BUHLES, M., EL GAMMAL, S., STÜCKER, M., PANZ, B., POPP, C., HOFFMANN, K., HAPPE, M. & ALTMEYER, P. (1994). The hyperperfusion of the psoriatic plaques correlates histologically with dilation of vessels. *Acta Derm. Venereol.* **S186,** 30–32.

BACHARACH-BUHLES, M., EL GAMMAL, S., PANZ, B. & ALTMEYER, P. (1994a). The pseudo-elongation of capillaries in psoriatic plaques. *Acta. Derm. Venereol.* (*Stockh*) **186,** 133–137.

BACHARACH-BUHLES, M., EL GAMMAL, S., PANZ, B. & ALTMEYER, P. (1994b). The topography of epithelium and vascular plexuses in psoriasis. In: Electron Microscopy in Dermatology—Basic and Clinical Research (Ishibashi, Y. Nakagawa, H. & Suzuki, H. eds), pp. 345–351. Amsterdam: Elsevier Science.

BACHARACH-BUHLES, M., EL GAMMAL, S., PANZ, B. & ALTMEYER, P. (1997). In psoriasis the epidermis, including the subepidermal vascular plexus, grows downwards into the dermis. *Br. J. Dermatol.* **136,** 97–101.

BHUSHAN, M., MCLAUGHLIN, B., WEISS, J. B. & GRIFFITHS, C. E. M. (1999). Levels of endothelial cell stimulating angiogenesis factor and vascular endothelial growth factor are elevated in psoriasis. *Br. J. Dermatol.* **141,** 1054–1060.

BRAVERMAN, I. M. & SIBLEY, J. (1982). Role of microcirculation in the treatment and pathogenesis of psoriasis. *J. Invest. Dermatol.* **78,** 12–17.

BULL, R. H., BATES, D. O. & MORTIMER, P. S. (1992). Intravital video-capillaroscopy for the study of the microcirculation in psoriasis. *Br. J. Dermatol.* **126,** 436–445.

BUTLER, A. R., MEGSON, I. L. & WRIGHT, P. (1998). Diffusion of nitric oxide and scavenging by blood in the vasculature. *BBA-Gen. Subjects* **1425,** 168–176.

CLIFF, S., BEDLOW, A. J., STANTON, A. W. B. & MORTIMER, P. S. (1999). An *in vivo* study of the microlymphatics in psoriasis using fluorescence microlymphography. *Br. J. Dermatol.* **140,** 61–66.

COBBOLD, C. A. & SHERRATT, J. A. (2000). Mathematical modelling of nitric oxide activity in wound healing can explain keloid and hypertrophic scarring. *J. theor. Biol.* **204,** 257–288.

CREAMER, D., ALLEN, M. H., SOUSA, A., POSTON, R. & BARKER, J. N. W. N. (1997a). Localization of endothelial proliferation and microvascular expansion in active plaque psoriasis. *Br. J. Dermatol.* **136,** 859–865.

CREAMER, D., JAGGER, R., ALLEN, M., BICKNELL, R. & BARKER, J. (1997b). Overexpression of the angiogenic factor platelet-derived endothelial cell growth factor/thymidine phosphorylase in psoriatic plaques. *Br. J. Dermatol.* **137,** 851–855.

CULOTTA, E. & KOSHLAND JR, D. E. (1992). NO news is good news. *Science* **258,** 1862–1865.

DENICOLA, A., SOUZA, J. M. & RADI, R. (1998). Diffusion of peroxynitrite across erythrocyte membranes. *Proc. Natl Acad. Sci. U.S.A.* **95,** 3566–3571.

DETMAR, M., BROWN, L. F., CLAFFEY, K. P., YEE, K. T., KOCHER, O., JACKMAN, R. W., BERSE, B. & DVORAK, H. F. (1994). Overexpression of vascular permeability factor/vascular endothelial growth factor and its receptors in psoriasis. *J. Exp. Med.* **180,** 1141–1146.

ELDER, J. T., FISHER, G. J., LINDQUIST, P. B., BENNETT, G. L., PITTELKOW, M. R., COFFEY, R. J., ELLINGSWORTH, L., DERYNCK, R. & VOORHEES, J. J. (1989). Overexpression of transforming growth factor alpha in psoriatic epidermis. *Science* **243,** 811–814.

ETTEHADI, P., GREAVES, M. W., WALLACH, D., ADERKA, D. & CAMP, R. D. R. (1994). Elevated tumour necrosis factor-alpha (TNF-α) biological activity in psoriatic skin lesions. *Clin. Exp. Immunol.* **96,** 146–151.

FRIEDL, P., ZÄNKER, K. S. & BROCKER, E. B. (1998). Cell migration strategies in 3D extracellular matrix: differences in morphology, cell matrix interactions, and integrin function. *Microsc. Res. Tech.* **43,** 369–378.

GOW, A. J. & STAMLER, J. S. (1998). Reactions between nitric oxide and haemoglobin under physiological conditions. *Nature* **391,** 169–173.

HAKIM, T. S., SUGIMORI, K., CAMPORESI, E. M. & ANDERSON, G. (1996). Half-life of nitric oxide in aqueous solutions with and without haemoglobin. *Physiol. Meas.* **17,** 267–277.

HIBBS, J. B., TAINTOR, R. R., VAVRIN, Z. & RACHLIN, E. M. (1989). Nitric oxide: a cytostatic activated macrophage effector molecule. *Biochem. Biophys. Res. Commun.* **157,** 87–94.

IGNARRO, L. J., BYRNS, R. E., BUGA, G. M. & WOOD, K. S. (1987). Endothelium-derived relaxing factor from pulmonary artery and vein possesses the pharmacologic and chemical properties identical to those of nitric oxide radical. *Circ. Res.* **61,** 866–879.

IRWIN, M., BRAVERMAN, M. D. & AGNES YEN, B. S. (1977). Ultrastructure of the capillary loops in the dermal papillae of psoriasis. *J. Invest. Dermatol.* **68,** 53–60.

KISSNER, R., NAUSER, T., BUGNON, P., LYE, P. G. & KOPPENOL, W. H. (1997). Formation and properties of peroxynitrite as studied by laser flash photolysis, high-pressure stopped-flow technique, and pulse radiolysis. *Chem. Res. Toxicol.* **10,** 1285–1292.

KLEMP, P. & STABERG, B. (1983). Cutaneous blood flow in psoriasis. *J. Invest. Dermatol.* **81,** 503–506.

KOLB-BACHOFEN, V., FEHSEL, K., MICHEL, G. & RUZICKA, T. (1994). Epidermal keratinocyte expression of inducible nitric oxide synthase in skin lesions of psoriasis vulgaris. *Lancet* **344,** 139.

KRISCHEL, V., BRUCH-GERHARZ, D., SUSCHEK, C., KRONCKE, K. D., RUZICKA, T. & KOLB-BACHOFEN, V. (1998). Biphasic effect of exogenous nitric oxide on proliferation and differentiation in skin derived keratinocytes but not fibroblasts. *J. Inves. Dermatol.* **111,** 286–291.

KROGSTAD, A. L., SWANBECK, G. & WALLIN, B. G. (1995). Axon-reflex-mediated vasodilation in the psoriatic plaque? *J. Invest. Dermatol.* **104,** 872–876.

KU, D. D. (1996). Nitric oxide- and nitric oxide-donor induced relaxation. *Meth. Enzymol.* **269,** 107–119.

LANCASTER, J. R. (1994). Simulation of the diffusion and reaction of endogenously produced nitric oxide. *Proc. Natl Acad. Sci. U.S.A.* **91,** 8137–8141.

LANCASTER, J. R. (1997). A tutorial on the diffusibility and reactivity of free nitric oxide. *Nitric Oxide*: *Biology and Chemistry* **1,** 18–39.

LAURENT, M., LEPOIVRE, M. & TENU, J. P. (1996). Kinetic modelling of the nitric oxide gradient generated *in vitro* by adherent cells expressing inducible nitric oxide synthase. *Biochem. J.* **314,** 109–113.

LIAO, J. C., HEIN, T. W., VAUGHN, M. W., HUANG, K. T. & KOU, L. (1999). Intravascular flow decreases erythrocyte consumption of nitric oxide. *Proc. Natl Acad. Sci. U.S.A.* **96,** 8757–8761.

LIU, X., MILLER, M. J. S., JOSHI, M. S., SADOWSKA-KROWICKA, H., CLARK, D. A. & LANCASTER JR, J. R. (1998). Diffusion-limited reaction of free nitric oxide with erythrocytes. *J. Biol. Chem.* **273,** 18 709–18 713.

LYMAR, S. V. & HURST, J. K. (1995). Rapid reaction between peroxonitrite ion and carbon-dioxide—implications for biological-activity. *J. Am. Chem. Soc.* **117,** 8867–8868.

MAEDA, H., OKAMOTO, T. & AKAIKE, T. (1998). Human matrix metalloprotease activation by insults of bacterial infection involving proteases and free radicals. *Biol. Chem.* **379,** 193–200.

MALINSKI, T., TAHA, Z., GRUNFELD, S., PATTON, S., KAPTURCZAK, M. & TOMBOULIAN, P. (1993). Diffusion of nitric oxide in the aorta wall monitored in situ by porphyrinic microsensors. *Biochem. Biophys. Res. Commun.* **193,** 1076–1082.

MONCADA, S. (1999). Nitric oxide: discovery and impact on clinical medicine. *J. Roy. Soc. Med.* **92,** 164–169.

NICKOLOFF, B. J., MITRA, R. S., VARANI, J., DIXIT, V. M. & POLVERINI, P. J. (1994). Aberrant production of interleukin-8 and thrombospondin-1 by psoriatic keratinocytes mediates angiogenesis. *Am. J. Pathol.* **144,** 820–828.

OKAMOTO, T., AKAIKE, T., NAGANO, T., MIYAJIMA, S., SUGA, M., ANDO, M., ICHIMORI, K. & MAEDA, H. (1997). Activation of human neutrophil procollagenase by nitrogen dioxide and peroxynitrite: a novel mechanism for procollagenase activation involving nitric oxide. *Arch. Biochem. Biophys.* **342,** 261–274.

OREM, A., ALIYAZICIOGLU, R., KIRAN, E., VANIZOR, B., CIMNOCODEIT, G. & DEGER, O. (1997). The relationship between nitric oxide production and activity of the disease in patients with psoriasis. *Arch. Dermatol.* **133,** 1606–1607.

ORMEROD, A. D., COPELAND, P. & SHAH, S. A. A. (2000). Treatment of psoriasis with topical N-G-monomethyl-L-arginine, an inhibitor of nitric oxide synthesis. *Br. J. Dermatol.* **142,** 985–990.

ORMEROD, A. D., WELLER, R., COPELAND, P., BENJAMIN, N., RALSTON, S. H., GRABOWSKI, P. & HERRIOT, R. (1998). Detection of nitric oxide and nitric oxide synthases in psoriasis. *Arch. Dermatol. Res.* **290,** 3–8.

SCHMIDT, K., DESCH, W., KLATT, P., KUKOVETZ, W. R. & MAYER, B. (1997). Release of nitric oxide from donors with known half-life: a mathematical model for calculating nitric oxide concentrations in aerobic solutions. *Naunyn-Schmiedebergs Arch. Pharmacol.* **355,** 457–462.

SHAH, M., FOREMAN, D. M. & FERGUSON, M. W. J. (1994). Neutralising antibody to TGF-$\beta_{1,2}$ reduces cutaneous scarring in adult rodents. *J. Cell Sci.* **107,** 1137–1157.

THIBODEAU, G. A. & PATTON, K. T. (1997). *The Human Body in Health and Disease.* St. Louis: Mosby Year Book, Inc.

UITTO, J. (1986). Interstitial collagens. In: *Biology of the Integument* 2: *Vertebrates* (Bereiter-Hahn, J. Matoltsy, A. G. & Richards, K. S. eds). pp. 800–809. Berlin: Springer-Verlag.

VAUGHN, M. W., KUO, L. & LIAO, J. C. (1998). Estimation of nitric oxide production and reaction rates in tissue by use of a mathematical model. *Am. J. Physiol.* **43,** H2163–H2176.

WELLER, R. & ORMEROD, A. (1997). Increased expression of nitric oxide synthase. *Br. J. Dermatol.* **136,** 132–148.

WELLER, R., ORMEROD, A. & BENJAMIN, N. (1996a). Nitric oxide generation measured directly from psoriatic plaques by chemiluminescence. *Br. J. Dermatol.* **134,** 569.

WELLER, R., PATTULLO, S., SMITH, L., GOLDEN, M., ORMEROD, A. & BENJAMIN, N. (1996b). Nitric oxide is generated on the skin surface by reduction of sweat nitrate. *J. Invest. Dermatol.* **107,** 327–331.

WHEATER, P. R., BURKITT, H. G., STEVENS, A. & LOWE, J. S. (1985). *Basic Histopathology:A Colour Atlas and Text.* London: Churchill Livingstone.

ZICHE, M., MORBIDELLI, L., MASINI, E., AMERINI, S., GRANGE, R. H. J., MAGGI, C. A., GEPPETTI, P. & LEDDA, F. (1994). Nitric-oxide mediates angiogenesis *in-vivo* and endothelial-cell growth and migration *in-vitro* promoted by substance-P. *J. Clin. Invest.* **94,** 2036–2044.

APPENDIX A

D_n, D_p: The diffusion coefficient for nitric oxide in intact tissue is roughly 3300 $\mu m^2 s^{-1}$ (Malinski *et al.*, 1993). Vaughn *et al.* (1998) give estimates for the diffusion coefficient between 2000 and 3400 $\mu m^2 s^{-1}$ from the data of Malinski *et al.* (1993). There is no experimental value for the diffusion coefficient of peroxynitrite. However, it has a similar permeability across phospholipid membranes as nitric oxide (Denicola *et al.*, 1998). Hence, its diffusion coefficient will be roughly similar to that of nitric oxide with some compensation for its larger mass. This compensation factor is $(15/31)^{1/3}$, giving a diffusion coefficient of roughly 2600 $\mu m^2 s^{-1}$.

λ, k_1, s: The rate constant for the reaction of nitric oxide with superoxide is 19 $nM^{-1} s^{-1}$ (Kissner *et al.*, 1997). The background removal rate of nitric oxide in tissue is roughly 0.17 s^{-1} (Lancaster, 1994). Vaughn *et al.* (1998) give estimates for the removal rate of between 0.006 and 0.01 s^{-1} from the data of Malinski *et al.* (1993). We do not have any estimate for the superoxide concentration in tissue. The reaction between NO and superoxide is very fast compared with other NO reactions. Thus, if we assume that this is the predominant reaction, the superoxide concentration should be $\sim$0.01 nM for a removal rate of 0.17 s^{-1}. Smaller superoxide concentrations will give correspondingly smaller peroxynitrite concentrations. Note that in model 1, $\lambda = k_1 s$.

d_1: Liu *et al.* (1998) found a decay rate of 385 s^{-1} for nitric oxide in blood. Independently, Hakim *et al.* (1996) found a maximum rate constant for nitric oxide and red blood cell haemoglobin of 2×10^5 $M^{-1} s^{-1}$. Taking a haemoglobin concentration in blood as 2 mM gives a maximum decay rate of 400 s^{-1}. However, Liao *et al.* (1999) showed that the rate constant in flowing blood is 5×10^4 $M^{-1} s^{-1}$, which is the value we use here, hence $d_1 = 100\ s^{-1}$.

d_2: In tissue, the dominant reaction of peroxynitrite is with carbon dioxide. This occurs at a rate of 5.8×10^4 $M^{-1} s^{-1}$ (Lymar & Hurst, 1995). The concentration of carbon dioxide is approximately 1 mM giving an approximate decay rate of peroxynitrite in tissue of 58 s^{-1}.

d_3: Denicola *et al.* (1998) measured the reaction rate for peroxynitrite and haemoglobin as 1.04×10^4 $M^{-1} s^{-1}$ at 25°C. This gives a decay rate of 20 s^{-1}; we take the value at body temperature to be $d_3 = 30\ s^{-1}$.

d_4: There is no experimental data for the removal rate of procollagenase, although we could expect it to be roughly on the order of a few minutes. We chose its value to be 0.01 s^{-1}.

d_5, k_2, k_3: Okamoto *et al.* (1997) performed *in vitro* studies on the peroxynitrite activation of neutrophil procollagenase. From their experimental set-up we constructed the following model:

$$\dot{p} = -k_2 p m' - dp + y(t), \tag{A.1}$$

$$\dot{m}' = -k_2 p m', \tag{A.2}$$

$$\dot{m} = k_2 p m' - d_5 m, \tag{A.3}$$

$$\dot{c} = -k_3 m c, \tag{A.4}$$

where

$$y(t) = 3a\delta(t - n\tau) \quad \text{for } n = 0, \ldots, \infty, \tag{A.5}$$

where $\delta(t)$ is the delta function. The initial conditions are $p(0) = 0$, $m'(0) = 0.6\ \mu M$, $m(0) = 0$ and $c(0) = 1.8\ \mu M$ and the known parameter values are $d = 0.7\ s^{-1}$, $a = 0.4$–$1200\ \mu M$ and $\tau = 300$ s. By solving the model and fitting the solution to their data we estimated the following parameter values: $k_2 = 10^{-5}\ nM^{-1} s^{-1}$ and $k_3/d_5 = 5 \times 10^{-4}\ nM^{-1}$. Assuming an inhibition rate of collagenase by TIMPs on the order of a few minutes, we set $d_5 = 0.01\ s^{-1}$ and hence $k_3 = 5 \times 10^{-6}\ nM^{-1} s^{-1}$.

a_3, d_6, F: The cell density of fibroblasts is about 10^{-8} cells μm^{-3} (Cobbold & Sherratt, 2000). The collagen density in normal skin is 536 $\mu g\ mg^{-1}$ dry weight (Shah *et al.*, 1994). From our model this means that $a_3/d_6 = 536$. The time taken for rete pegs to return to normal from psoriatic skin is of the order of weeks. This implies a regrowth time for collagen of about 10^6 s. From eqn (6) the regrowth time is of the order $536/(a_3 F)$. Hence, we take $a_3 = 5.36 \times 10^4$ $\mu g\ mg^{-1}\ \mu m^3\ s^{-1}\ cell^{-1}$ and $d_6 = 100\ s^{-1}$.

$a_2 L$: To estimate the term $a_2 L$ we note that the rate of degradation of collagen is given by the

factor $k_3 m$ in eqn (6). The time-scale for this is on the order of a few days, therefore $k_3 m \sim 10^{-5}\,\mathrm{s}^{-1}$. At equilibrium, $m^* = k_2\, a_2 L p^*/(d_4 d_5)$ by assuming that $k_2 p^* \ll d_4$. The value of p^* is taken from the epidermal–dermal junction when the basal cells are far from the capillaries. From the 1D simulations this value is 0.12 before the basal cells have moved towards the capillary. This gives a value of roughly $170\,\mathrm{nM\,s}^{-1}$ for $a_2 L$.

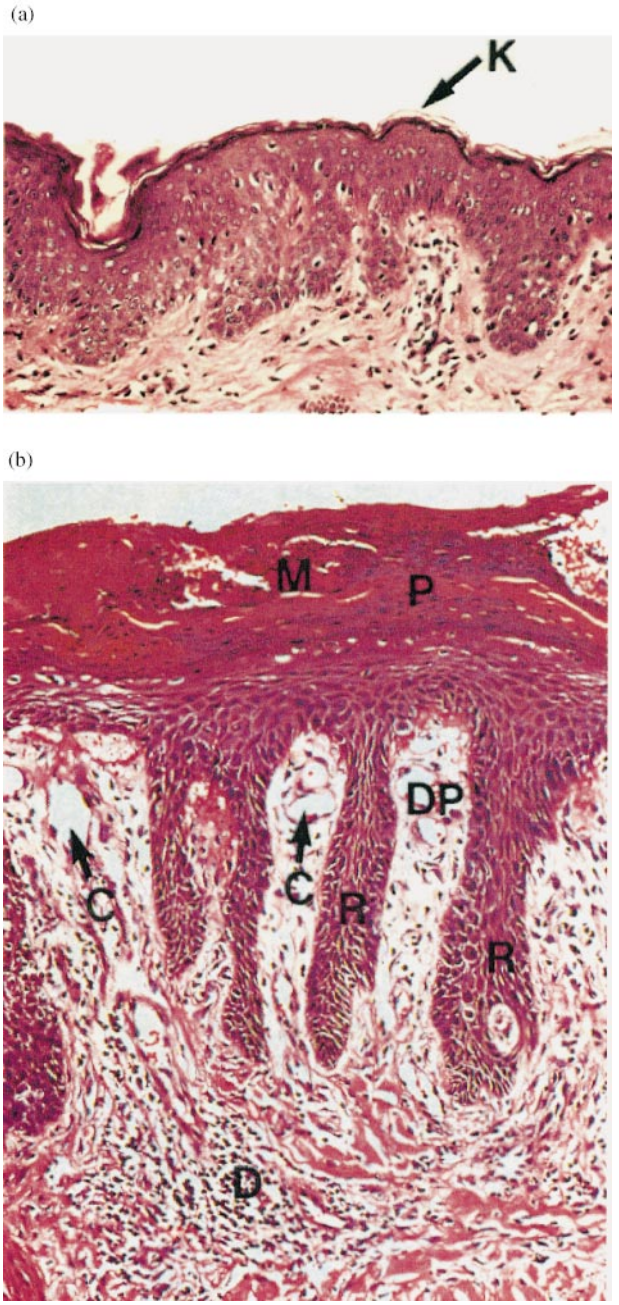

FIG. 1. (a) Normal skin showing the lightly stained dermis, the medium stained epidermis and the darkly stained dead outer layer of cells. (b) Skin from a psoriatic plaque with elongated narrow rete pegs (R). Between the rete pegs, the epidermis is thinned over oedematous and prominent dermal papillae (DP) in which dilated capillaries are prominent (c). The epidermis contains small aggregations of neutrophils forming microabscesses (M). There is a variable chronic inflammatory infiltrate in the upper dermis (D). Kindly reproduced from Wheater *et al.* (1985).

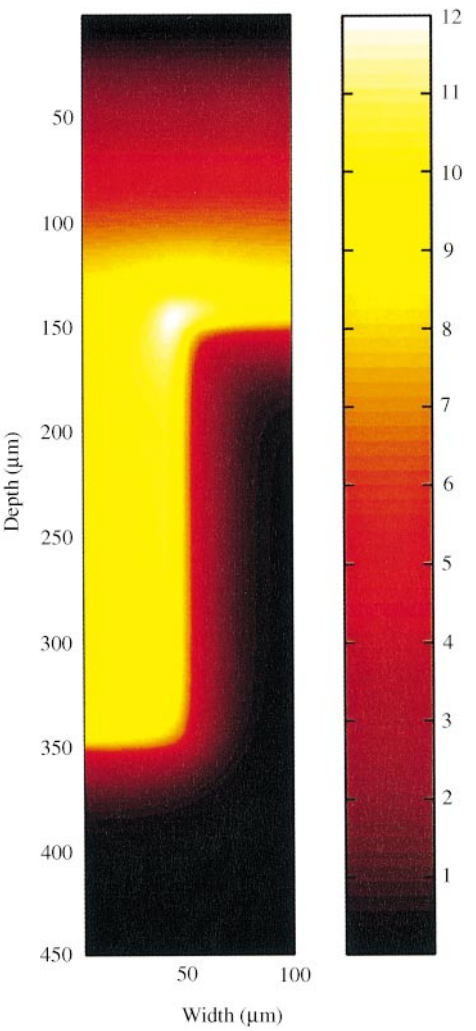

FIG. 3. Example of the steady-state solution of nitric oxide (model 1). The skin surface is at the top. The solution is calculated using the alternating-direction-implicit method with $\delta t = 2 \times 10^{-3}$ s and $\delta x = \delta y = 1\,\mu$m. Equilibrium is reached within a few seconds. The colour-bar gives the nitric oxide concentration in nM.

doi:10.1006/jtbi.2001.2400

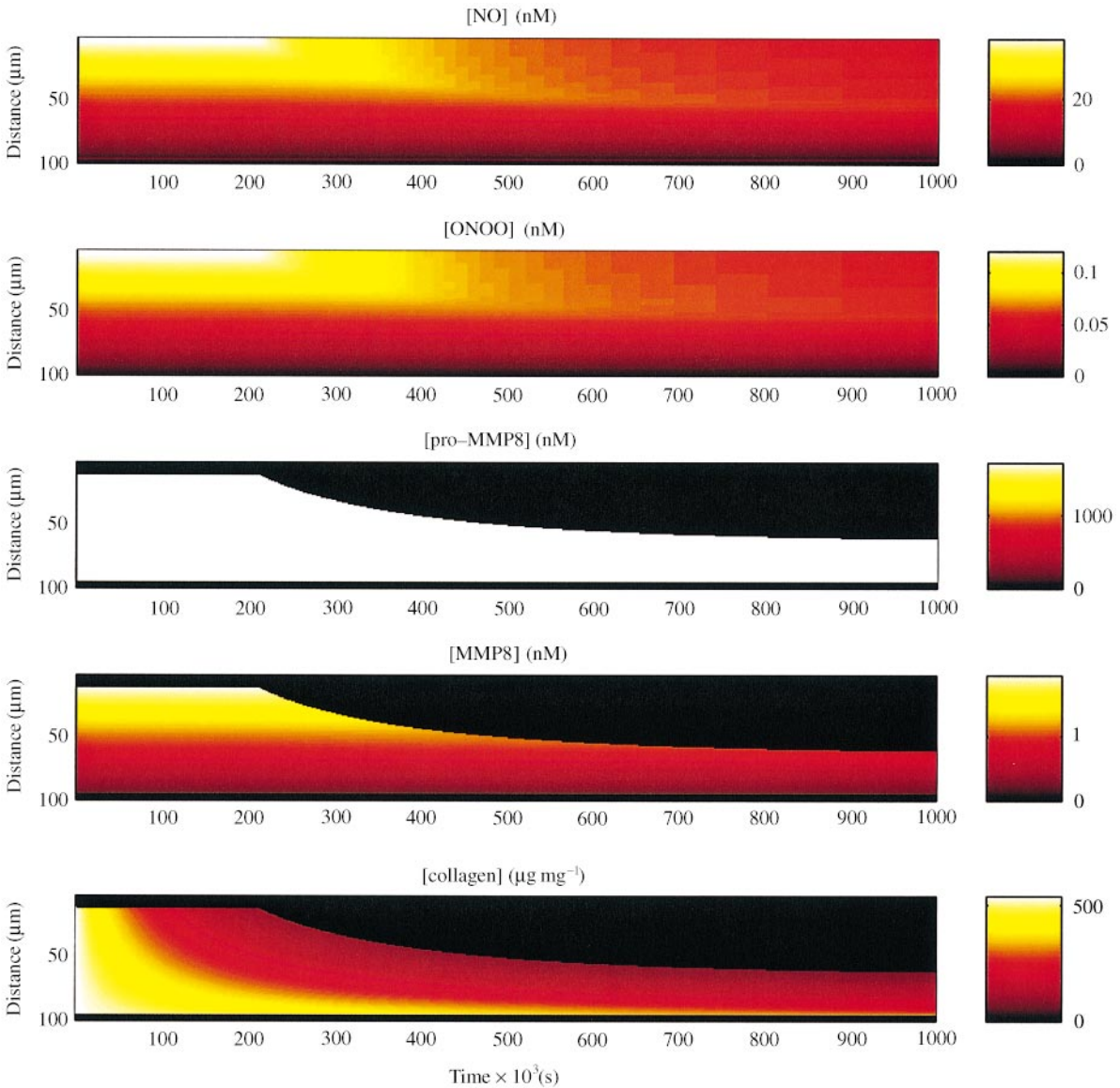

FIG. 6. Space–time plots of the solution to eqns (2–6). The basal layer initially starts at the top boundary and moves downwards towards the capillary at the bottom boundary. Nitric oxide and peroxynitrite diffuse throughout the whole of space, whereas proMMP-8, MMP-8 and collagen only exist in the dermis, hence, the black regions above the basal layer in the bottom three graphs. The numerical method used was Crank–Nicholson with $\delta t = 10^{-2}$ s and $\delta x = 1$ μm. No flux boundaries were used at both ends.

doi:10.1006/jtbi.2001.2400

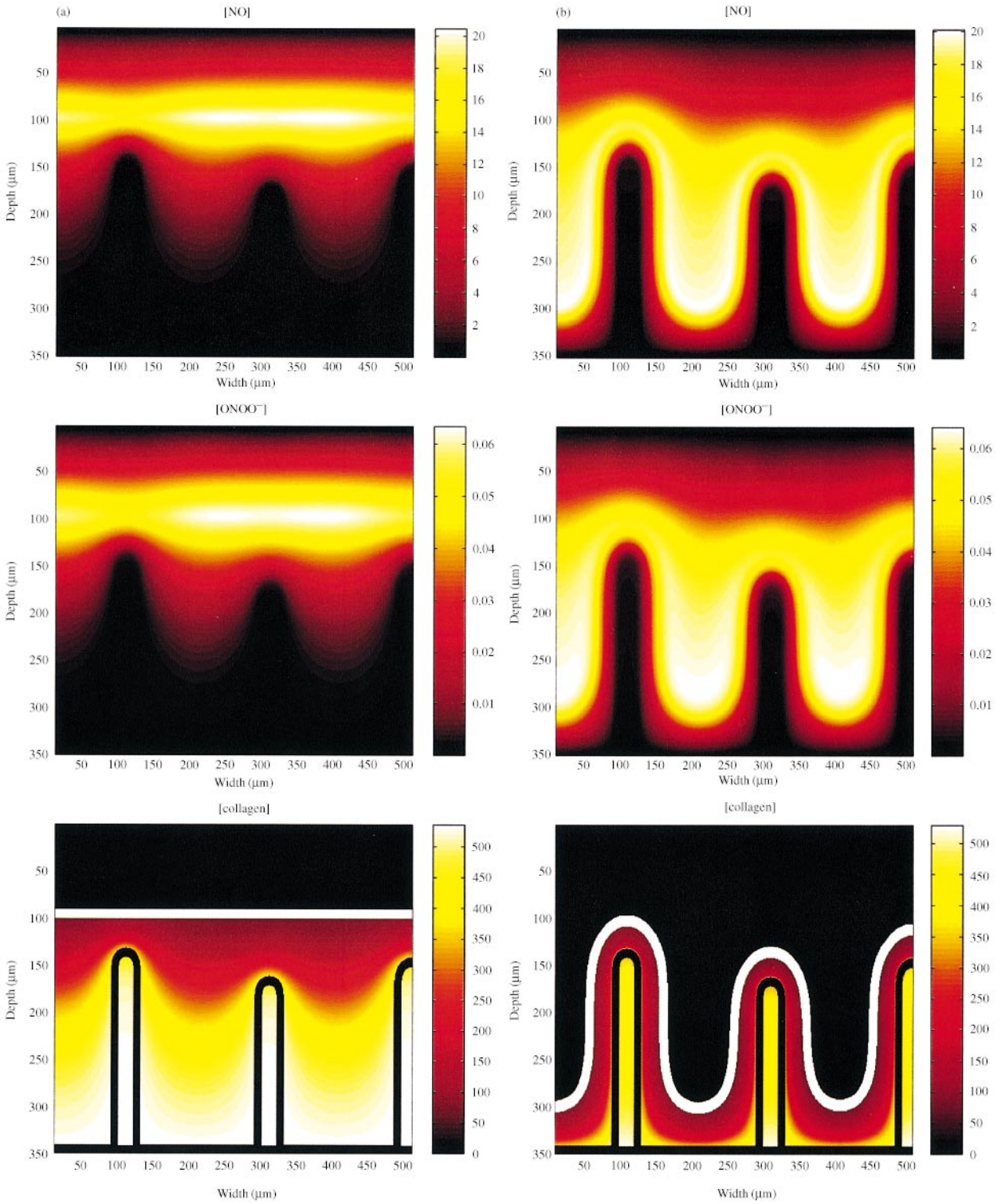

FIG. 9. The two-dimensional solution of eqns (2–6). The position of the basal layer is represented as the white band and the capillaries are in black in the bottom two plots. (a) The initial configuration of basal layer and capillaries with a new configuration of the basal layer is about to be computed because collagen density has fallen below the critical threshold. (b) The final configuration with no more movement of the basal layer is possible. The numerical method for the solution of nitric oxide and peroxynitrite is ADI with $\delta t = 5 \times 10^{-3}$ s and $\delta x = \delta y = 1$ μm. Once these solutions have equilibrated the proMMP $-$ 8 and MMP $-$ 8, spatial concentrations are calculated from eqns (7) and (8). The collagen density is then solved over time using a first-order Runge–Kutta algorithm with $\delta t = 500$ s and a spatial resolution of 1 μm^2. Movies of this simulation can be downloaded from http://www.ma.hw.ac.uk/ $\sim$ njs/psoriasis.html.

doi:10.1006/jtbi.2001.2400